7-1-1995

Modeling the Lower Chesapeake Bay Littoral Zone & Fringing Wetlands:Ecosystem Processes and Habitat Linkages.I. Simulation Model Development and Description

Christopher P. Buzzelli
Virginia Institute of Marine Science

Richard L. Wetzel
Virginia Institute of Marine Science

Mark B. Meyers
Virginia Institute of Marine Science

Modeling the Lower Chesapeake Bay Littoral Zone & Fringing Wetlands: Ecosystem Processes and Habitat Linkages

I. Simulation Model Development and Description

by

Christopher P. Buzzelli, Richard L. Wetzel and Mark B. Meyers

An Annual Report Submitted to

United States Environmental Protection Agency
Region III
Chesapeake Bay Program Office
410 Severn Avenue
Annapolis, Maryland 21403

Special Report No. 334
in Applied Marine Science and Ocean Engineering

School of Marine Science / Virginia Institute of Marine Science
College of William and Mary
Gloucester Point, VA 23062

July 1995

Modeling the Lower Chesapeake Bay Littoral Zone & Fringing Wetlands: Ecosystem Processes and Habitat Linkages.

I. Simulation Model Development and Description

by

Christopher P. Buzzelli, Richard L. Wetzel and Mark B. Meyers

An Annual Report Submitted to

United States Environmental Protection Agency
Region III
Chespeake Bay Program Office
410 Severn Avenue
Annapolis, Maryland 21403

Special Report No. 334
in Applied Marine Science and Ocean Engineering

School of Marine Science / Virginia Institute of Marine Science
College of William & Mary
Gloucester Point, VA 23062

July 1995

INTRODUCTION

The development and testing of ecological, process-oriented simulation models has been undertaken as part of the Chesapeake Bay Program with particular regard to living marine resources. The research and modeling studies accomplished to date as well as those studies proposed for continuing work will enhance our basic understanding of natural processes and anthropogenic influences that control important natural, living resources. In addition, the results bear directly on the development of effective management strategies for the conservation of natural resources and their long-term survival. These ecosystem process modeling efforts also address in ways the larger scale, water quality and hydrodynamic modeling efforts can not, the development of specific habitat criteria and management strategies. Coupling these efforts with past and continuing efforts in water quality and hydrodynamic modeling will provide both scientist and manager with a powerful suite of tools for estuarine and coastal systems analysis.

The estuary is conceptualized as being composed of three, interacting large-scale components: uplands, wetlands and aquatic or open-water systems. The interaction between these components is governed primarily by large-scale hydrologic and meteorologic natural forcings, and by human perturbations. Within these components are smaller-scale units defined or identified by their ecological/biological structure and organized by the flow of energy, the cycling of essential elements, and the controls imposed by physical, chemical, and biological interactions, including those imposed by human activity. Examples of such units include wetland and submersed aquatic vegetation (SAV) habitats, littoral zones, open water, and benthic environments. It is at this fundamental habitat level of ecological organization that our modeling efforts have been and continue to be focused. The development of a large-scale, fully-integrated ecosystem model of the estuary, though a goal to work toward, is beyond the scope of the present effort. The development and implementation of the models as exemplified in this report are necessary steps toward designing and building in the future integrated, large-scale ecosystem models of the estuary and its tributaries.

Our previous work has focused on the development and simulation analysis of SAV models and conceptual modeling of emergent intertidal marsh communities. The SAV models have clearly shown the importance of environmental factors (submarine light, temperature) and biological factors (epiphytic fouling, grazing) for controlling SAV growth, distribution, and long-term population survival. The SAV stand-alone model has proved an accurate predictor of water quality-SAV response and habitat criteria for SAV survival. We have over this past year revised and expanded this model to include other components of the littoral zone. This effort will make it easier to relate "littoral processes"–which includes the benthos, SAV, and pelagic habitats–to models of hydrodynamics and water quality extant for Chesapeake Bay and its major tributaries.

The focus of the efforts for this period has been on the development, calibration, validation, and preliminary simulation analysis of ecosystem process models for specific, highly-distributed components of the estuary emphasizing intertidal wetlands, SAV habitat, and other

principal components of the littoral zone. We have refined and implemented the conceptual models of the principal habitats of the littoral zone into numerical simulation models. Incorporating spatially-varying information, such as salinity, nutrient concentration, and bathymetry as forcings can suggest how SAV-driven, phytoplankton-driven, and detrital and benthic microflora-driven food webs function along the tributaries and into Chesapeake Bay. One of our goals has been to formulate both spatially- and temporally-varying forcings in ways which will enable the incorporation of biological productivity and biologically-driven elemental cycling (*e.g.*, for carbon, oxygen, and nitrogen) into larger-scale, water quality and hydrodynamic models.

This report describes our efforts over the period of May 1994 to May 1995 to develop, implement and analyze ecosystem process models for littoral zone areas including fringing wetlands of the lower Chesapeake Bay.

RELATION TO WQ-HD MODELING EFFORT

Cooperation between the Modeling and Living Resources Subcommittees over the past few years has lead to significant advances in the ability of the Chesapeake Bay Program's eutrophication modeling package to resolve and address living resource and habitat questions. Specifically, the enhancements under development include the addition of submerged aquatic vegetation (SAV), benthic algae, benthic macrofauna, and zooplankton. Their inclusion represents successful cooperation between scientists and managers involved in both living resource and water quality issues.

Enhancements of model applications developed under the Living Resources Subcommittee's Ecosystem Process Modeling Program have also benefited from this collaboration. A specific example is the use of temperature and dissolved oxygen output from the hydrodynamic model component for indirect coupling with the fish bioenergetics models (Brandt et al. 1995). In addition to providing stand-alone model solutions to habitat and resource questions, the Ecosystem Process Modeling Program has established a role of testing enhancements (new formulations, additional trophic levels, and biological-physical couplings) on smaller scale models prior to implementation within the eutrophication model package.

In this vein, we have coupled SAV-littoral zone and emergent marsh habitat models with a tidal exchange model in order to explore the interactions of adjacent intertidal and shallow subtidal zones for predicting water quality, system productivity and resource utilization. These modeling activities at the smaller scale of the littoral zone are essential in that they represent boundary conditions for the larger scale modeling efforts. The models in particular provide linkages between traditional water quality models and ecological processes on time and space scales relevant to specific habitats and target species.

OVERVIEW & RATIONALE FOR LITTORAL ZONE MODELING EFFORT

Background

Although approximately 40% of the subtidal area of the Chesapeake Bay is $\leq$ 2.0 m below MLW, littoral zone ecosystems historically have not been included in efforts to simulate bay wide environmental processes (Kuo and Park, 1995; Spinner, 1969) The littoral zone environments of the Chesapeake Bay exhibit patterns of aquatic productivity, sediment processes, and biogeochemical cycling distinct from those of adjacent channel environments (Kuo and Park, 1995; Malone, 1986). Few published studies have utilized mechanistic models to analyze habitat interactions among coastal ecosystem components in order to identify the probable linkages to other areas of the landscape (Boumans and Sklar, 1990; Childers, 1993; Costanza, 1990). It is important to provide mechanistic models to help address issues related to environmental change in coastal environments (Costanza, 1990; Wetzel and Hopkinson, 1990). Understanding of the synergistic interactions among littoral zone habitats provides an essential link between the preservation of environmental quality and the protection of living resources such as macrophyte communities and fishery species (Dennison, 1993; Heck and Thoman, 1984; Kneib and Wagner, 1994).

Estuarine landscapes are a mosaic of subtidal and intertidal vegetated and nonvegetated habitats including photic sandy shoals, seagrass meadows, mudflats, and low and high marshes (Correll *et al.*, 1992). The estuarine flank environments exhibit bi-directional exchange of channel derived inorganic nutrients and shoal derived particulate materials (Kuo and Park, 1995; Malone, 1986). The considerable shoal regions of the Chesapeake Bay are bounded by fringing estuarine marshes which abut a comparatively steep mainland slope and are eroding through wave effects at the edges, subsurface peat breakdown, and internal ponding (Finklestein and Hardaway, 1988; Stevenson, 1988). Depending upon the configuration of the landscape the various littoral zone ecosystem components possess different biogeochemical connections through meteorologic and hydrodynamic forces (Correll *et al.*, 1992; Vorosmarty and Loder, 1994). In particular, ecosystems that contain irregularly inundated marshes can display periodicity in patterns of water chemistry and discharge to the adjacent habitats (Vorosmarty and Loder, 1994). The exchanges (imports or exports) of inorganic or organic materials (dissolved or particulate) between marshes and the surrounding estuary depends upon the overall developmental marsh history and resulting basin hydroperiod (Childers, 1993).

Each of the different littoral zone habitats can have a suite of different primary producers including water column phytoplankton, sediment microalgae, seagrasses and attached epiphyte communities, and marsh grasses. Submarine irradiance along with other meteorologic (seasonality in temperature and rainfall) and hydrodynamic (nutrient run-off and river flow) factors significantly influence estuarine phytoplankton processes (Mallin, 1994). Sediment microalgae contribute significantly to primary production in nonvegetated and vegetated subtidal environments in many ecosystems including those in Massachusetts (Gould and Gallagher, 1990),

South Carolina (Pinckney and Zingmark, 1993), Mississippi (Moncreiff, 1992; Sullivan and Moncreiff, 1988), Denmark (de Jonge and Colijn, 1994; Sand-Jensen and Borum, 1991). Sediment microalgae also play a significant role in the fluxes of oxygen and nutrients across the sediment-water interface (Rizzo, 1992; Sundback and Graneli, 1988). Seagrass meadows are complex and productive littoral zone ecosystem components (Moncreiff, 1992; Murray and Wetzel, 1987; Roman, 1990; Sand-Jensen and Borum, 1991). Seagrass meadows can serve as indicators of water quality because the plants and attached epiphytes are sensitive to submarine light attenuation and the concentrations of chlorophyll a, suspended sediments, and inorganic nutrients (Bach, 1993; Dennison, 1993; Wetzel and Neckles, 1986). Salt marshes are areas of increased rates of productivity and nutrient cycling (Childers, 1993; Dame and Kenny, 1986; Pinckney and Zingmark, 1993) although there few studies have focused upon the estuarine fringing wetlands of Chesapeake Bay (Drake and Read, 1981; Gross, 1991; Wolaver *et al.*, 1983). Dynamic modeling offers the opportunity to include all of the different phototrophs in an analysis of primary production and water quality over multiple habitats in the littoral zone.

Different approaches have been employed to mathematically model stocks and processes in coastal ecosystems. Approaches include but are not limited to empirical modeling using regression (Dame, 1991) or other matrix methods (Dennison, 1993; Keller, 1989), network analysis (Baird and Ulanowicz, 1989), dynamic budgeting (Childers, 1993), mechanistic modeling of dynamic interactions (Bach, 1993; Christian and Wetzel, 1991; Wetzel and Hopkinson, 1990), and combinations of several approaches (Morris, 1982; Morris *et al.*, 1984). These various studies address specific aspects of individual primary producers in the littoral zone. None of the studies listed have included suites of primary producers within a variety of hydrodynamically linked habitats. Mechanistic simulation provides the opportunity to organize information and initiate research and can be joined with geographic techniques to provide a framework in which to investigate dynamic coastal landscapes (Childers, 1993; Christian and Wetzel, 1991; Costanza, 1990; Lee, 1992).

This report is a technical summary describing the development of a series of dynamic models created to simulate water column processes and sediment primary production in littoral zone habitats characteristic of the lower Chesapeake Bay and its tributary estuaries. These models have been developed as heuristic tools to integrate investigative methods (field and geographic data collection), to link distinct aquatic habitats within the ecosystem mosaic, and to link water quality and living resources in the ecosystem.

Methods

Reference Area (Habitats)

The Goodwin Islands National Estuarine Research Reserve (GI NERR) is an 800 hectare (ha) littoral zone ecosystem at the mouth of York River in lower Chesapeake Bay (37° 12' 46" N,

76° 23' 46" W; Fig 1). The islands are owned by the College of William and Mary and are managed by the Chesapeake Bay National Estuarine Research Reserve System in Virginia (CBNERRS-VA) of the National Oceanic and Atmospheric Administration (NOAA). The research reserve includes the islands and a buffer zone that extends out to the -2.0 m depth contour (MLW). The GI NERR is an oblong island system with a large subtidal shoal extending between the shoreline and the -2.0 m (MLW) depth contour. Between -1.0 and -0.5 m (MLW) is approximately 120 hectares of subtidal seagrass mostly comprised of eelgrass (*Zostera marina* L). There is approximately 100 hectares of nonvegetated intertidal habitats with fine sands and silty sediments that surround 90 hectares of intertidal marsh vegetated primarily by *Spartina alterniflora* although there are regions vegetated by *Spartina patens* and *Distichlis spicata* and *Juncus roemerianus*. The intertidal marsh grades into a salt bush habitat that includes the *Iva frutescens* and *Baccharis halimifolia* and the largest island has a small amount of maritime forest and upland vegetated by red oak, loblolly pine, black gum, and cottonwood (J. Perry, pers. Comm). Intertidal and subtidal habitat patterns vary over time (seasonally-interannually) and space (10's-100's ha). Historical aerial photography depicts long term persistence and resilience in the GI NERR eelgrass meadows but overall erosion and some horizontal migration for intertidal marshes.

Model Background

Four concentric primary habitat types were identified and include (1) nonvegetated subtidal (NVST; 420 ha), (2) vegetated subtidal (VST; 120 ha), (3) nonvegetated intertidal (NVIT; 100 ha), and (4) vegetated intertidal (VIT; 85 ha) (Fig. 2). These four habitats were selected based upon abiotic and biotic characteristics relative to the elevation gradient along which they are located (Fig. 3). Figure 4 depicts the generalized conceptual diagrams for each of the 4 habitat models that were based upon the four habitat types. The global forcing functions are tidal water level, irradiance, and water temperature. The subtidal and intertidal nonvegetated models each have 7 state variables including large and small phytoplankton size classes (diatoms and other plankton, respectively), labile and refractory particulate organic carbon (LPOC and RPOC), dissolved organic carbon (DOC), and total dissolved inorganic nitrogen (TDIN) and sediment microalgae (SM) (Table 1). In addition to these 7 state variables the vegetated subtidal and intertidal habitat models include additional state variables in the forms of epiphyte carbon (ZepiC) and shoot and root-rhizome carbon and nitrogen of *Zostera marina* or *Spartina alterniflora* (ZSC, ZSN, ZRRC, ZRRN, SSC, SSN, SRRC, SRRN; Table 1). An Euler integration routine is used with an integration interval (dt) for the subtidal habitat models of 0.03125 d while intertidal habitat models use 0.0078125 d. Simulations can span 1-10 years of model time.

Hydrodynamic Model Design

The four habitat simulation models are linked by tidal exchange across the boundaries of a sequence of boxes representing the NVST, VST, NVIT, and VIT habitats (Fig. 4). The habitat boxes fill and drain in consecutive order with the output from one providing the input for the next

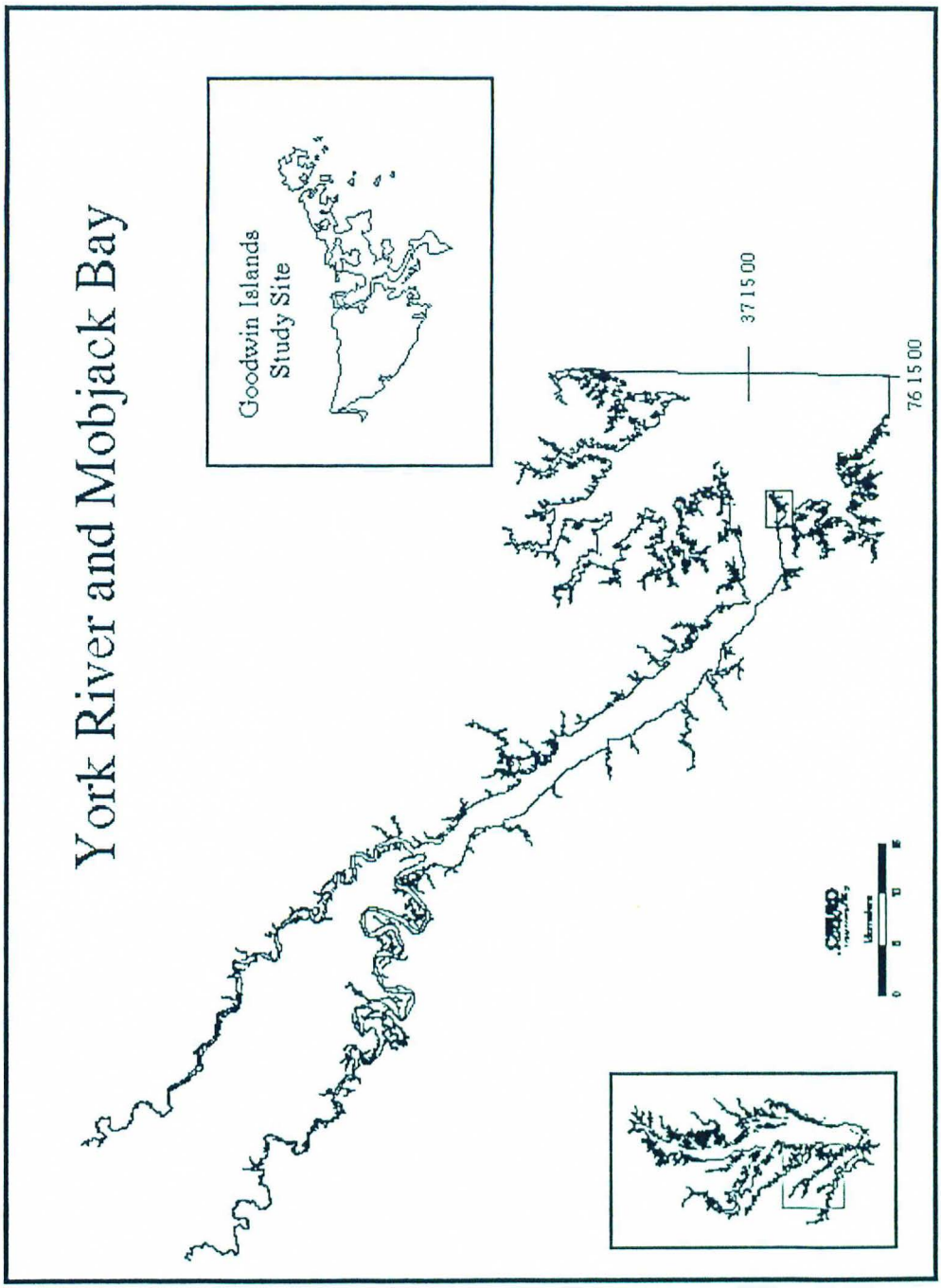

Figure 1. Location map for York River and Goodwin Islands Ecosystem

Figure 2. A generalized habitat map for the Goodwin Islands Ecosystem. The four habitats were delineated according to elevation and biotic characteristics.

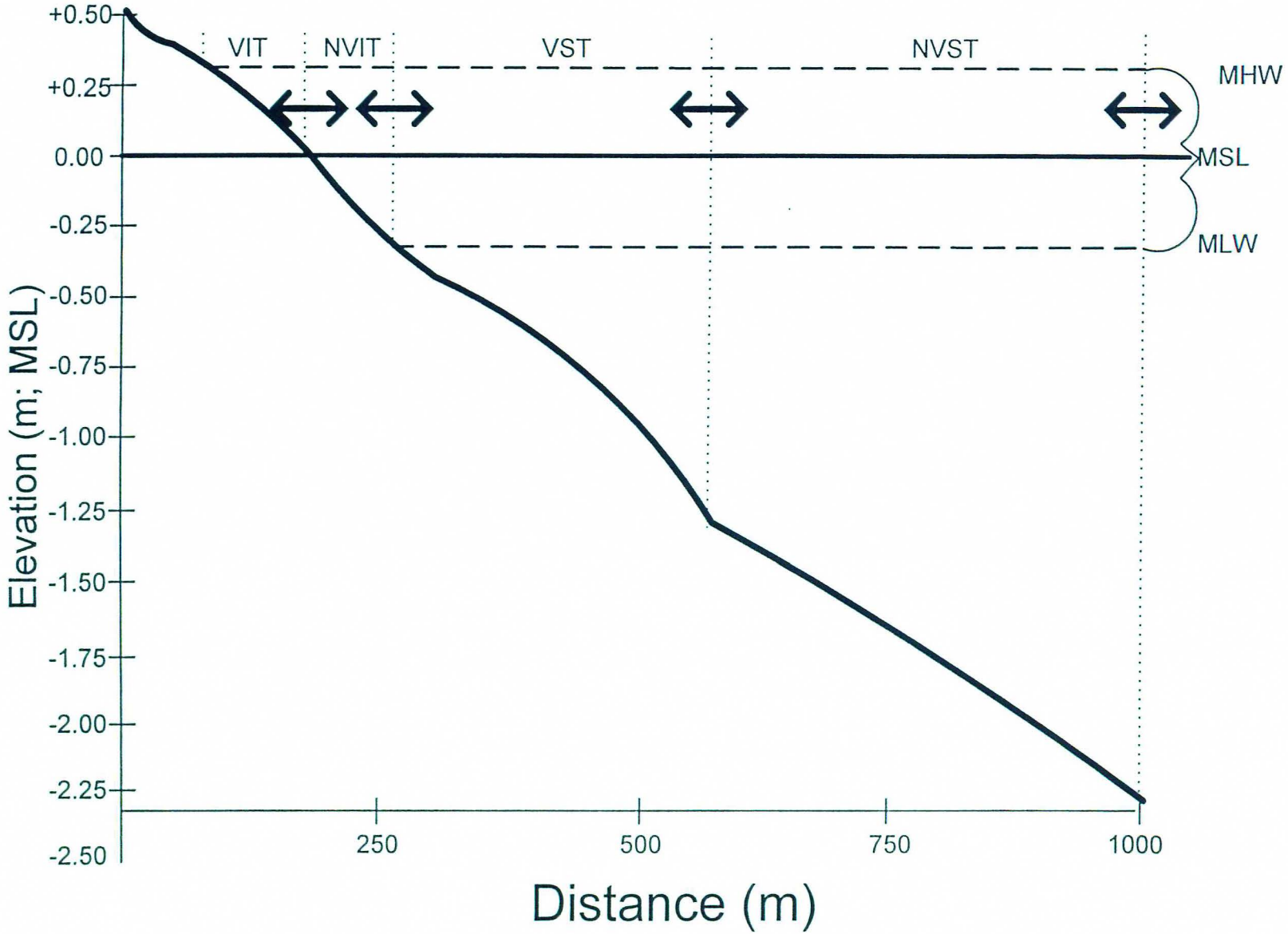

Figure 3. Two-dimensional profile of the Goodwin Islands Ecosystem. The vertical scale is elevation in meters relative to mean sea level (MSL). The horizontal scale is exaggerated to show the offshore distance of each delineated habitat. The four habitat abbreviations are shown. The interhabitat exchanges are depicted by the large two headed arrows that span over the habitat boundaries.

Table 1. List of state variables for habitat models. Each habitat model includes the first 7 state variables listed. In addition to the basic seven the vegetated subtidal habitat model (VST) includes those related to Zostera marina while the vegetated intertidal habitat model (VIT) has those related to Spartina alternilflora.

ABBREV.	DESCRIPTION	UNITS
DIA	Diatom Carbon Mass	gC
OP	Other Plankton Carbon Mass	gC
LPOC	Labile Particulate Organic Carbon	gC
RPOC	Refractory Particulate Organic Carbon	gC
DOC	Dissolved Organic Carbon	gC
TDIN	Total Dissolved Inorganic Nitrogen	μM
SM	Sediment Microalgae	gC m^{-2}
ZSC	Zostera marina Shoot Carbon	gC m^{-2}
ZSN	Zostera marina Shoot Nitrogen	gN m^{-2}
ZRRC	Zostera marina Root-Rhizome Carbon	gC m^{-2}
ZRRN	Zostera marina Root-Rhizome Nitrogen	gN m^{-2}
ZepiC	Zostera marina Epiphytic Biomass	gC m^{-2}
SSC	Spartina alterniflora Shoot Carbon	gC m^{-2}
SSN	Spartina alterniflora Shoot Nitrogen	gN m^{-2}
SRRC	Spartina alterniflora Root-Rhizome Carbon	gC m^{-2}
SRRN	Spartina alterniflora Root-Rhizome Nitrogen	gN m^{-2}

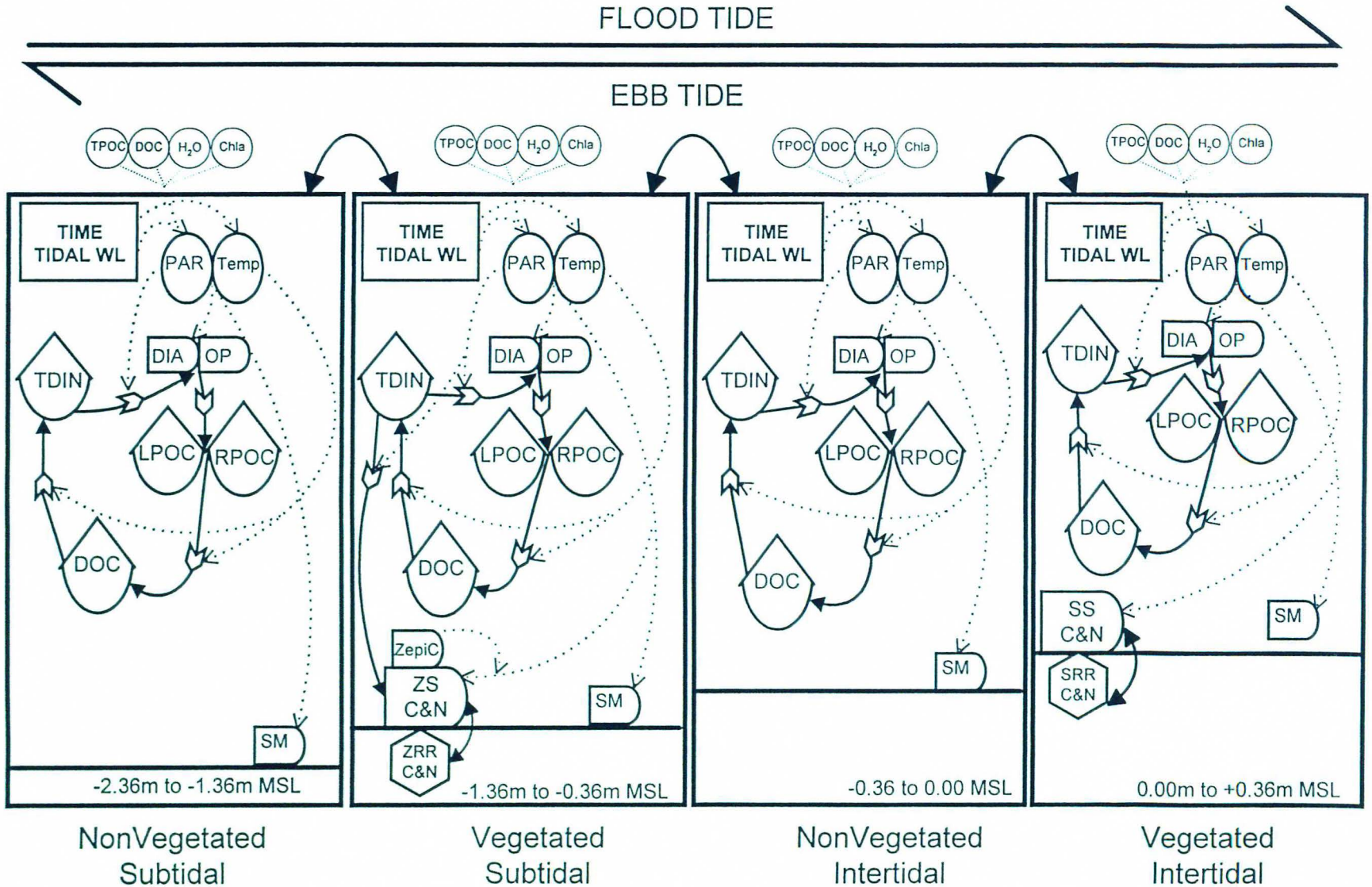

Figure 4. Generalized conceptual diagram for the four habitat models. Dashed lines are information flow while solid lines with workgates represent mass flows. Model time, tidal water level, photosynthetically active radiation (PAR), and water temperature (Temp) influence the six water column state variables (DIA, OP, LPOC, RPOC, DOC, TDIN). The two phytoplankton size classes and the two POC fractions are shown as paired state variables. Each model also includes sediment microalgae (SM). The vegetated subtidal and intertidal models have Zostera marina and Spartina alterniflora shoot and root-rhizome carbon and nitrogen, respectively

in the sequence. The nonvegetated subtidal is bounded by an unlimited source/sink representing the offshore channel while the vegetated marsh is bounded by the upland with no exchange across the upland boundary. Watershed exchanges are assumed to be zero because the Goodwin Islands have little upland and are isolated from the mainland though exchange could be easily implemented if a terrestrial linkage is desired. The habitat volume changes each dt and flux equations for water column masses (see phytoplankton below) were derived using finite difference solutions to equations for the exchange of conservative substances between a channel and an adjacent control volume in both flood and ebb situations (K. Park, pers. comm). This approach assumes no diffusion, no advection, and the water within each box is totally homogeneous during each time step. The change in tidal height each time step is multiplied by habitat wet area to derive the changes in habitat volumes used in the simulation of water column processes. While subtidal habitat wet areas are constant (see Appendix B), intertidal habitat wet areas are derived using a hypsometric curve. This study uses hypsometry because it provides a concise method in which to represent the cumulative characteristics of basin morphology (Friedrichs and D. G. Aubrey, 1994; Strahler, 1952). The area-height relationship of a hypsometric curve provides a better approximation for basin inundation regimes than a linear 2-D profile (Fig. 3) because it includes the effects of shoreline curvature (Boon and Byrne, 1981; Friedrichs and D. G. Aubrey, 1994) and hypsometric determination of inundation can be useful in the analysis of wetland biogeochemical cycling (Childers, 1993; Eiser and Kjerve, 1986).

The tidal exchange equations for a constituent, e.g., chlorophyll *a*, of mass M_i where the subscript I = {1,..,4} represents each of four habitats, are given below. Note that m_i is total habitat mass; concentration units are calculated as M_i * h(t)*A(t), where (t) indicates that these are time varying quantities and that the wetted area A(t) is constant for the subtidal habitat, but variable for the intertidal habitats. The tidally varying water height is represented by h, referenced to mean sea level, and its change from one model time step to the next is represented as Δh. Other processes affecting state variable masses are growth or biochemical production (α), losses from biological uptake or mortality and/or grazing (m) and exchanges with the benthos (b). In the present model, I=0 represents the channel boundary condition. Figures 4 and 5 illustrate the spatial relationships between the habitats.

$$\frac{\Delta M_i}{\Delta t} = (\alpha - m)\cdot M_i + \left[\frac{C_k\cdot\Delta h}{\Delta t} + b\right]\cdot A_i(t) \quad \begin{cases}\Delta h>0\ (flood)\text{: } k=i-1\\ \Delta h<0\ (ebb)\text{: } k=i\end{cases}$$

State Variables: Mathematical Structure

Table 2 contains the system of differential equations used to model the changes in the state variables listed in Table 1. Primary production (gC m^{-2} or m^{-3} d^{-1}) is modeled using the rates of

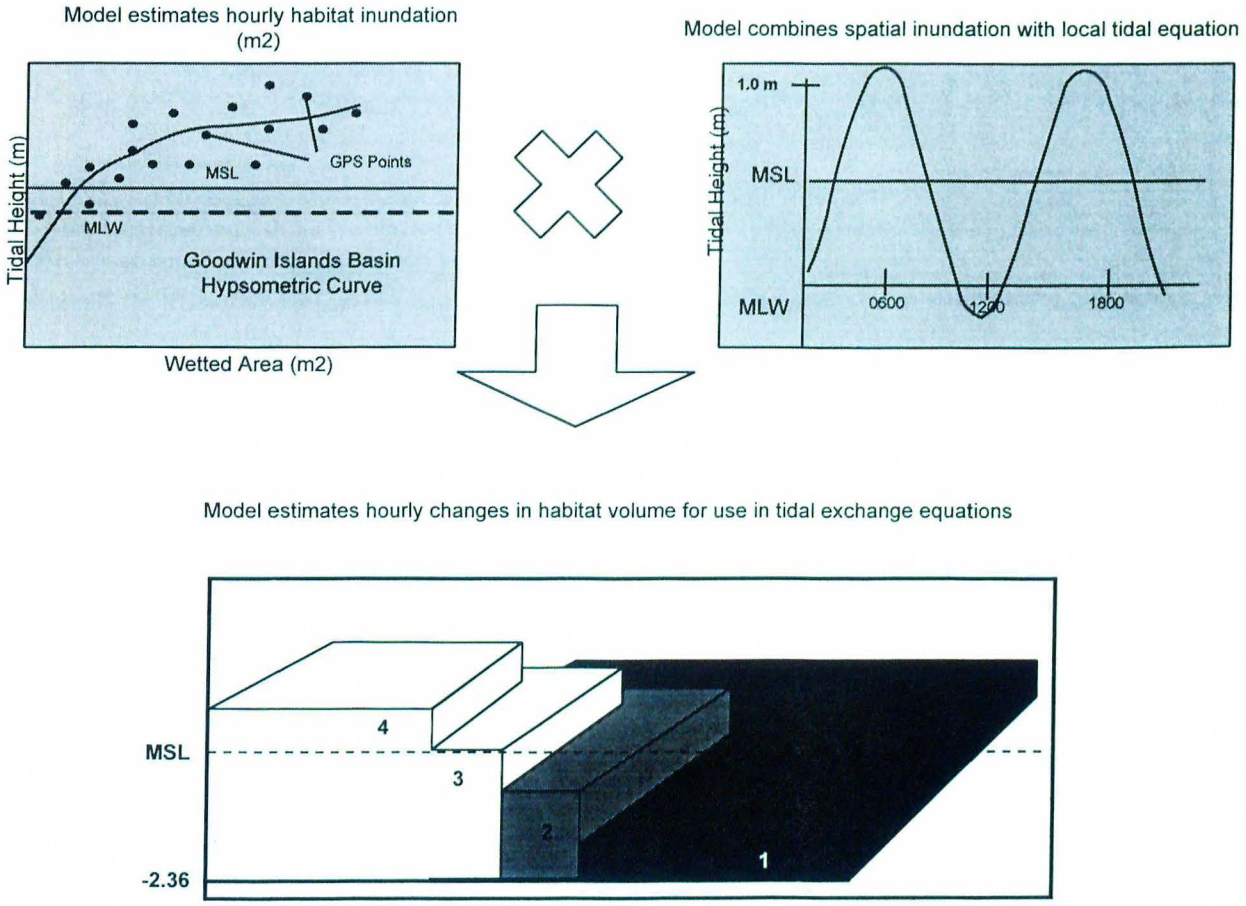

Figure 5. Output from the hypsometric model (m2) are combined with tidal height (m) to derive changes in volume (m3) for each of the littoral zone habitat models

Table 2. System of differential equations for state variables listed in Table 1.

Diatom Carbon Mass (gC)

$$DIA_{hab(t)} = DIA_{(t-dt)} + (DIA_{prod} - DIA_{resp} - DIA_{mort} - DIA_{exu} - DIA_{sed} \pm DIA_{flxab} \pm DIA_{flxbc}) * dt$$

Other Plankton Carbon Mass (gC)

$$OP_{hab(t)} = OP_{(t-dt)} + (OP_{prod} - OP_{resp} - OP_{mort} - OP_{exu} - OP_{sed} \pm OP_{flxab} \pm OP_{flxbc}) * dt$$

Labile Particulate Organic Carbon (gC)

$$LPOC_{hab(t)} = LPOC_{(t-dt)} + (LPOC_{prod} - LPOC_{hydrol} - LPOC_{setl} \pm LPOC_{flxab} \pm LPOC_{flxbc}) * dt$$

Refractory Particulate Organic Carbon (gC)

$$RPOC_{hab(t)} = RPOC_{(t-dt)} + (RPOC_{prod} - RPOC_{hydrol} - RPOC_{setl} \pm RPOC_{flxab} \pm RPOC_{flxbc}) * dt$$

Dissolved Organic Carbon (gC)

$$DOC_{hab(t)} = DOC_{(t-dt)} + (DOC_{prod} - DOC_{remin} \pm DOC_{flxab} \pm DOC_{flxbc}) * dt$$

Total Dissolved Inorganic Nitrogen (μM)

$$TDIN_{hab(t)} = TDIN_{(t-dt)} + (TDIN_{prod} - TDIN_{uptake} \pm TDIN_{swflx} \pm TDIN_{flxab} \pm TDIN_{flxbc}) * dt$$

Sediment Microalgae (gC m^{-2})

$$SMC_t = SMC_{(t-dt)} + (SMC_{prod} - SMC_{resp} - SMC_{los} - SMC_{res}) * dt$$

Zostera marina Shoot Carbon (gC m^{-2})

$$ZSC_t = ZSC_{(t-dt)} + (ZSC_{prod} - ZSC_{resp} - ZSC_{los} - ZC_{trans}) * dt$$

Zostera marina Shoot Nitrogen (gN m^{-2})

$$ZSN_t = ZSN_{(t-dt)} + (ZSN_{uptake} + ZN_{trans} - ZSN_{los}) * dt$$

Zostera marina Root-Rhizome Carbon (gC m^{-2})

$$ZRRC_t = ZRRC_{(t-dt)} + (ZC_{trans} - ZRRC_{resp} - ZRRC_{los} - ZRRC_{bed}) * dt$$

Zostera marina Root-Rhizome Nitrogen (gN m^{-2})

$$ZRRN_t = ZRRN_{(t-dt)} + (ZRRN_{uptake} - ZN_{trans} - ZRRN_{los} - ZRRN_{bed}) * dt$$

Zostera marina Epiphytic Biomass (gC m^{-2})

$$ZepiC_t = ZepiC_{(t-dt)} + (ZepiC_{prod} - ZepiC_{resp} - ZepiC_{graz} - ZepiC_{los}) * dt$$

Spartina alterniflora Shoot Carbon (gC m^{-2})

$$SSC_t = SSC_{(t-dt)} + (SSC_{prod} - SSC_{resp} - SSC_{los} \pm SC_{trans}) * dt$$

Spartina alterniflora Shoot Nitrogen (gN m^{-2})

$$SSN_t = SSN_{(t-dt)} + (SN_{trans} - SSN_{los}) * dt$$

Spartina alterniflora Root-Rhizome Carbon (gC m^{-2})

$$SRRC_t = SRRC_{(t-dt)} + (SC_{trans} - SRRC_{resp} - SRRC_{los} - SRRC_{bed}) * dt$$

Spartina alterniflora Root-Rhizome Nitrogen (gN m^{-2})

$$SRRN_t = SRRN_{(t-dt)} + (SRRN_{uptake} - SN_{trans} - SRRN_{los} - SRRN_{bed}) * dt$$

gross production, respiration, and loss through mortality or grazing (Table 2). Phytoplankton (DIA and OP) are also influenced by exudation, sedimentation, and transport to adjacent habitats (Table 2). The mathematical representations of the basic metabolic rate processes in diatoms, other plankton, sediment microalgae, and *Spartina alterniflora* are all similar and the DIA examples are provided in Appendix A. Appendix B contains all of the parameters, constants, and boundary conditions of the four habitat models. Gross production is affected by temperature, irradiance, and dissolved inorganic nitrogen (Appendix A). Respiration follows an exponential relationship with temperature (Cerco and Cole 1994). Production and mortality are represented by Gaussian functions with temperature (Cerco and Cole 1994). Phytoplankton exudation and sedimentation are also modeled according to Cerco and Cole (1994). Sediment microalgae are lost through resuspension and are grazed with the square of the biomass (Appendix A). The formulations for carbon productivity by *Zostera marina* and its epiphytes have been provided elsewhere (Wetzel and Neckles 1986; Wetzel and Meyers 1994). Nitrogen uptake by the shoots and root-rhizomes of *Zostera marina* are modeled using Michaelis-Menten kinetics limited by feedback functions based on the maximum and minimum nitrogen contents of the tissues (Appendices A and B). *Zostera marina* shoots and root-rhizomes maintain C:N ratios through the proportional nitrogen loss terms. Nitrogen is translocation only from root-rhizomes to shoots in order to meet shoot nitrogen demand (Appendix A). Nitrogen translocation is also limited by feedback functions based on the maximum and minimum nitrogen contents of the tissues. The formulations for nitrogen state variables of *Spartina alterniflora* are similar to those of *Zostera marina* except that there is no shoot uptake of nitrogen in *Spartina alterniflora*.

Water column particulate organic carbon (POC; gC m^{-3}) is influenced by production, hydrolysis, settling, and exchange between adjacent habitats (Table 2). POC is produced from phytoplankton and a fractional loss term added to that gained through resuspended sediment microalgae (Appendices A and B). POC is divided into labile and refractory fractions and rates of hyrolysis are calculated using an exponential relationship with temperature (Cerco and Cole 1994). LPOC and RPOC both settle from the water column and are exchanged laterally (Appendix A). DOC is influenced by production, remineralization, and exchange with adjacent habitats (Table 2). Hydrolyzed POC provides the DOC production rate while the remineralization rate is controlled by a temperature function and the refractory DOC fraction (Appendix B; Cerco and Cole 1994). Water column TDIN (mmoles m^{-3}) is influenced by production, autotrophic uptake, sediment-water fluxes, and exchange with adjacent habitats (Table 2). Production is calculated using the DOC remineralization rate and the C:N ratio of dissolved organic matter (Appendices A and B). TDIN is removed from the water column through uptake by phytoplankton in all habitat models and by *Zostera marina* in the vegetated subtidal habitat model (Appendix A). TDIN is exchanged vertically between the sediment and the overlying water column based upon rates determined from core incubations (C.P. Buzzelli, unpubl. data).

Preliminary Model Output

The model is presently being calibrated with data obtained by an intensive monitoring program within SAV habitat (Moore et al 1994). Preliminary output is presented to show the

behavior of the model and its applicability to both salt marsh and SAV habitat issues. For the nominal case (1993 conditions), the fortnightly behavior during an April simulation is a combination of both diurnal and tidal effects. Diurnal effects include primary production, nutrient uptake and dissolved organic matter production by both particulate organic matter breakdown and exudation by algae versus remineralization of dissolved organic matter, mortality of plant matter (including grazing losses), and respiration. Tidal effects of exchanges between adjacent habitats (including the channel boundary) are evident, especially the result of a spring-neap cycle (Figs. 6 and 7). Model output is presently being analyzed for the relative influences of within-habitat biogeochemical processes versus between-habitat tidal exchanges on the signals of water quality parameters evident in simulations and in high-frequency observations (Moore et al. 1994).

On a longer time scale, modeled annual cycles of sediment autotrophic biomass (sediment microalgae, eelgrass, and salt marsh cordgrass) are shown in Figure 8. Sediment microalgae in all four habitats show a relatively small range of annual variation (two-fold) in biomass and have similar cycles and biomasses across habitats. Furthermore, microalgal populations within vegetated habitats do not appear to be significantly shaded by macrophytes. Note that the apparent thickness of the microalgal biomass lines results from diurnal variations in biomass. The modeled algal populations have the potential to double in <3 days. Daily photosynthesis is roughly balanced over a 24-hr period by respiratory and mortality (predominantly grazing) losses, thus creating noticeable diurnal fluctuations, while yielding the noted small annual range. This contrasts with the slow, but highly seasonal accumulation of macrophyte biomass. Observed seasonality of sediment microalgae from the Goodwin Islands (Fig. 9) show little variation. However, a distinct late spring and summer minimum is evident which is not well reproduced by the model. Sensitivity analysis of the model (results not shown) suggests that this cannot be produced by moderate changes in the terms controlling photosynthesis or respiration. It is more likely that seasonally varying grazing pressure by the benthos, not yet included in the model, keeps sediment microalgal populations under tight control. We are investigating ways to parameterize this in the current model. Future versions may have explicitly modeled benthic grazers.

Eelgrass (*Zostera marina*) aboveground biomass (shoots) peaks in June and rapidly diminishes during July as a result of heat stress and leaf sloughing. There is a secondary fall peak followed by senescent loss. Below ground biomass (root and rhizome) accumulates during both productive periods (spring and fall). The modeled biomass compares well with observed biomass at Goodwin Islands (Fig. 9) in terms of both magnitude and seasonality.

Salt marsh cordgrass (*Spartina alterniflora*) aboveground biomass disappears completely during the winter (Fig. 8). Spring production is initiated from Below ground storage and subsequent primary production. While total biomass accumulates into summer, Below ground biomass builds during spring and diminishes somewhat during summer. The observed data from Goodwin Islands and other temperature salt marshes show a similar pattern. Aboveground biomass accumulates slowly throughout a long growing season. Investment in Below ground biomass is high, with above:below-ground ratios of approximately 1:3-1:5. The model captures this dynamic, though with some mid-summer loss of Below ground mass related to temperature-

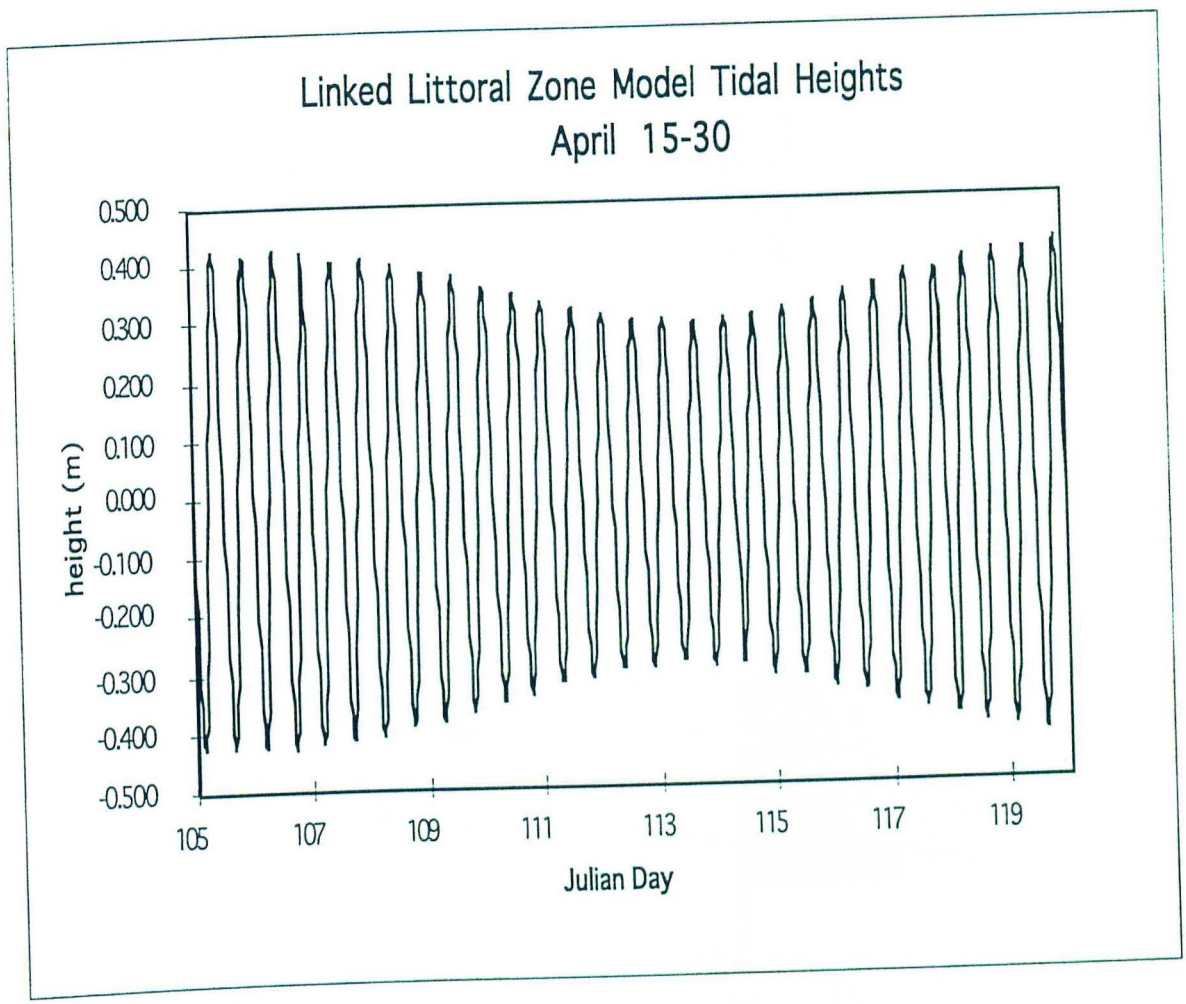

Figure 6. Simulated tidal height (m) for a fifteen day period in April 1993.

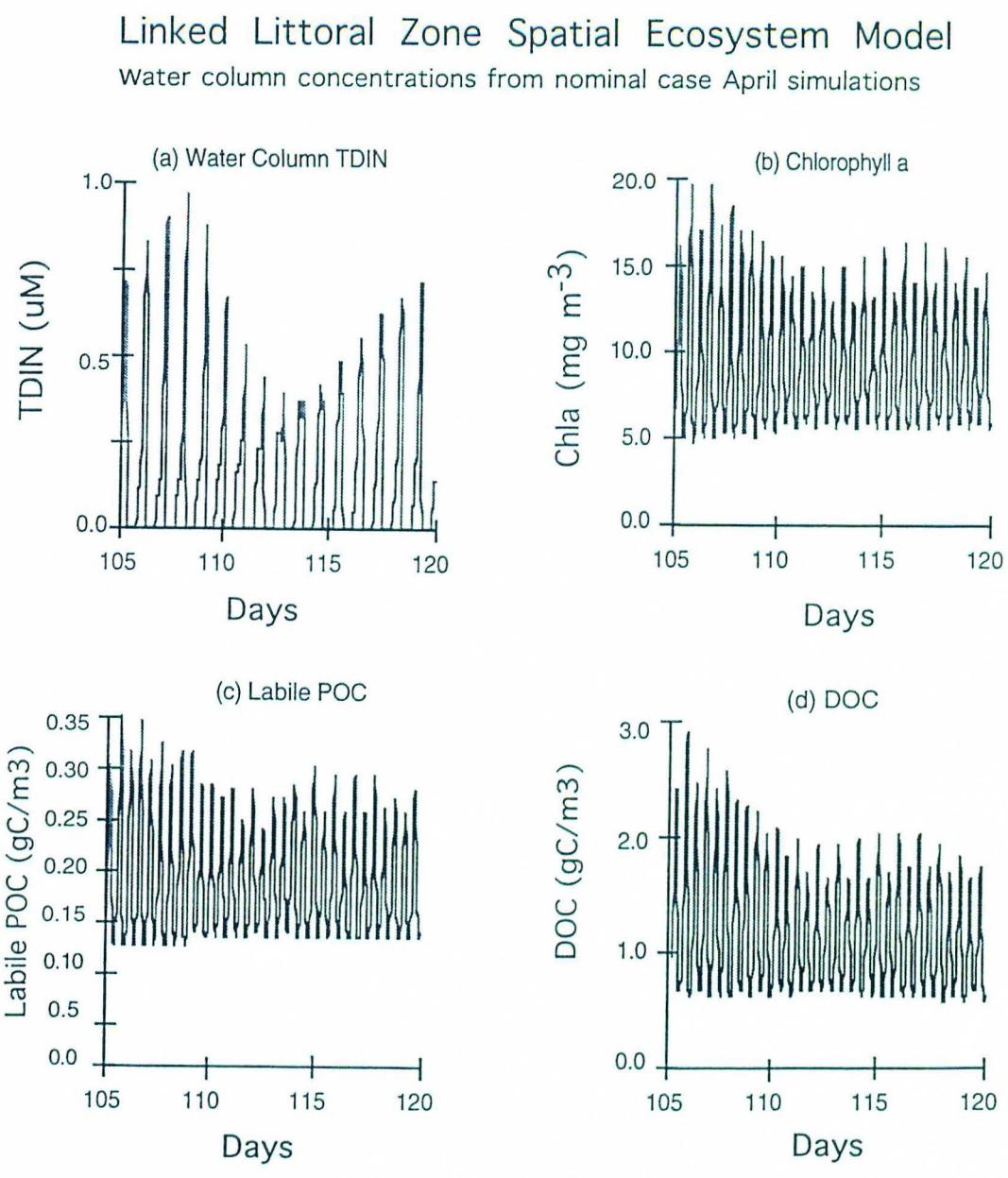

Figure 7. Fifteen day model output from April demonstrating changes in water column concentrations of (a) total dissolved inorganic nitrogen (μM), (b) phytoplankton chlorophyll *a* (mg m-3), (c) suspended labile particulate organic carbon (gC m-3), and (d) dissolved organic carbon (gC m-3) for the vegetated subtidal habitat model.

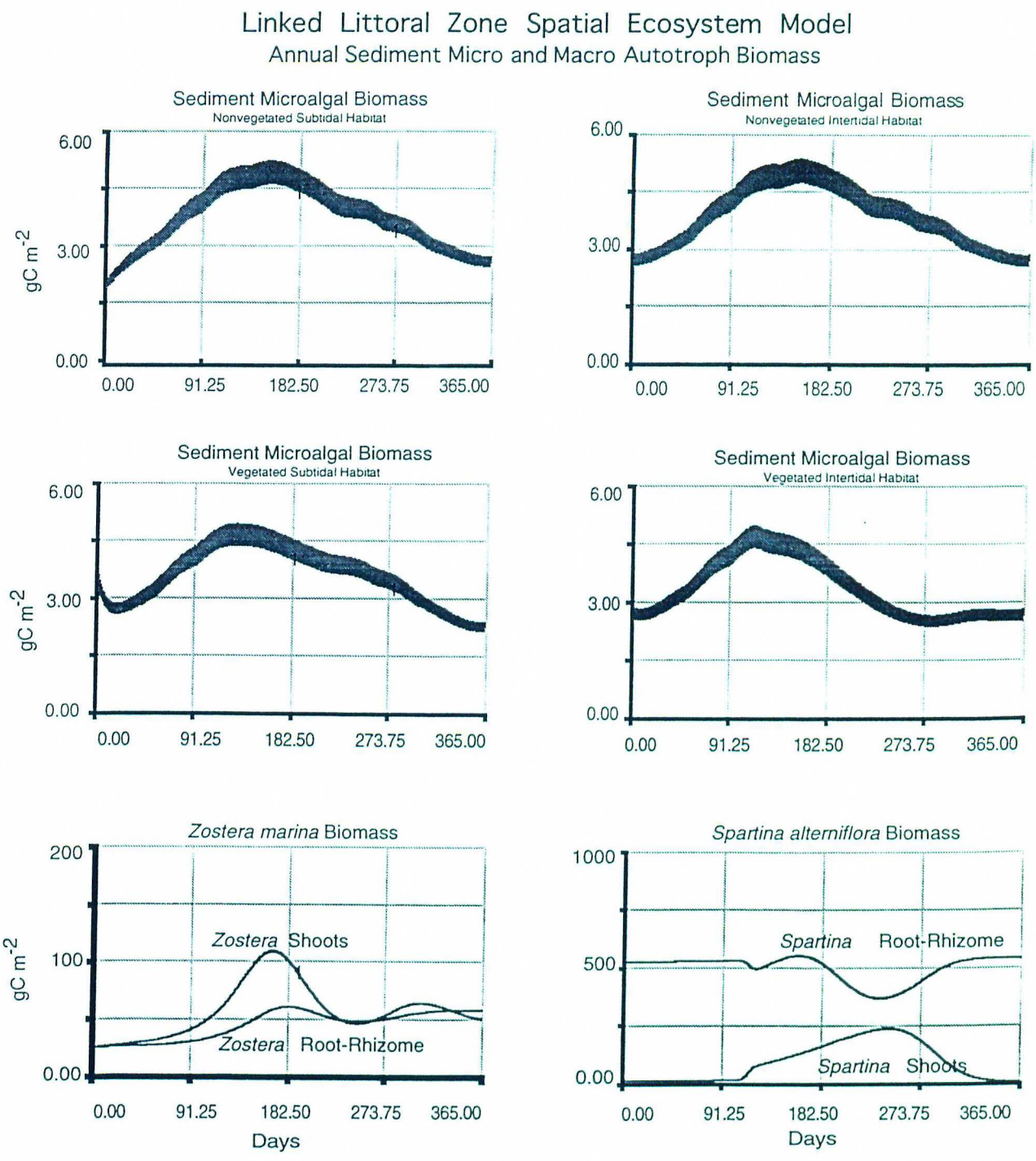

Figure 8. Modeled annual cycles of sediment microalgal biomass. The thickness evident in algal biomass plot lines result from diurnal fluctuations in biomass (see text). *Zostera marina* and *Spartina alterniflora* shoot and root-rhizome biomasses are shown.

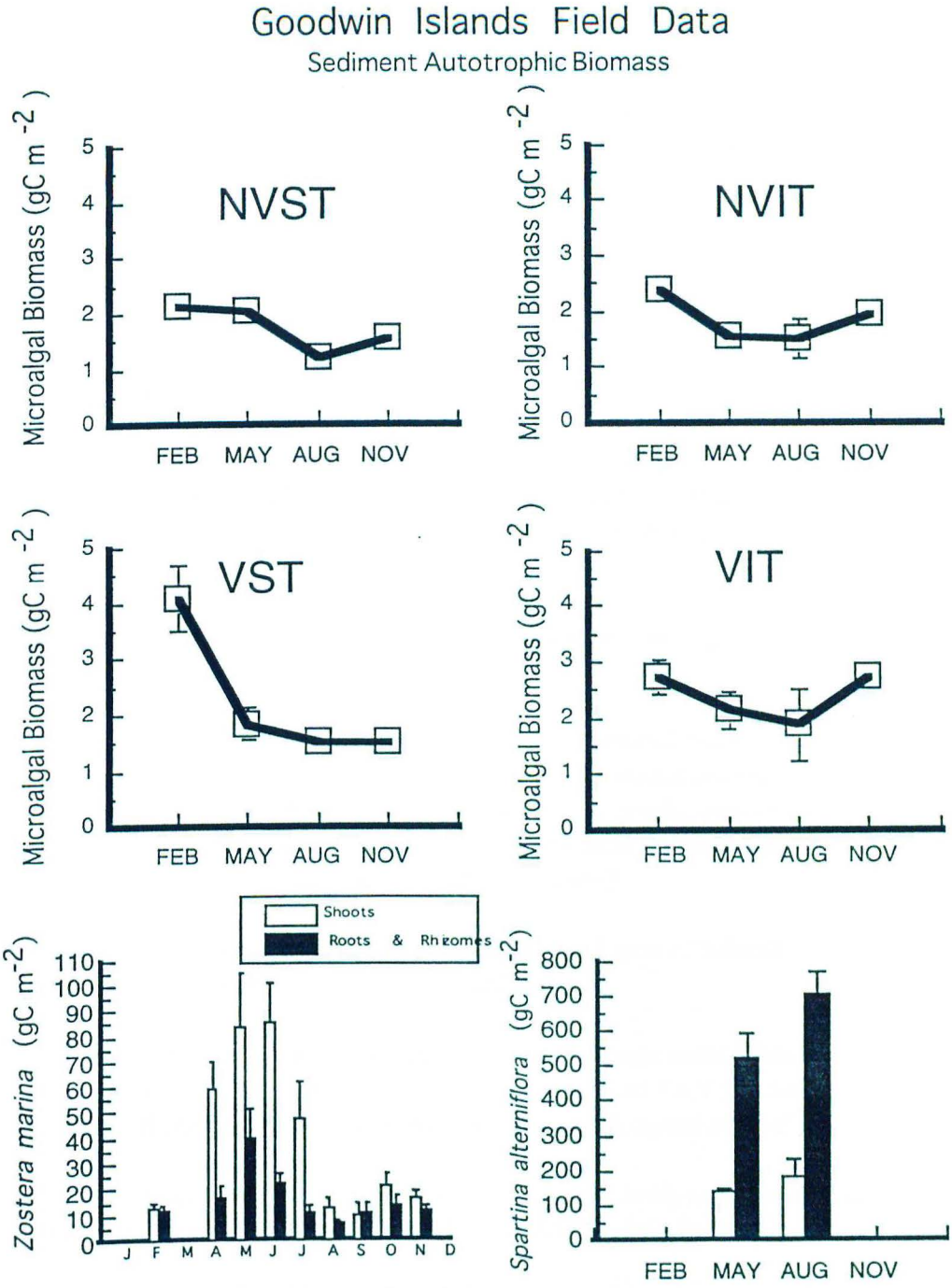

Figure 9. Observed sediment microalgal and macrophyte biomass from the Goodwin Islands National Estuarine Research Reserve. *Zostera marina* data are from 1993 (courtesy of K. Moore, VIMS). Microalgal and *Spartina alterniflora* data are from 1994-1995 (C. Buzzelli, SMS-VIMS).

dependent respiration rates.

Further comparisons with productivity and remineralization rates and checks for long term stability of the model are being performed before calibration is completed. Following calibration, scenario runs will include testing the impacts on water quality, production and survival of eelgrass and cord grass and the subsequent availability of food and habitat availability for higher trophic levels. Scenarios will be driven by altering boundary water quality conditions, matching historic and targeted restoration levels of nutrients, and by altering areas of adjacent habitat (marsh and SAV).

Management Implications and Future Directions

This ecosystem model links water quality and living resource dynamics in the littoral zone habitats that are essential to the survival of ecologically, commercially, and recreationally important juvenile and adult fishes and invertebrates. This approach affords the opportunity to investigate the potential effects of habitat alteration (e.g., changes in relative area of marsh or SAV beds), channel water quality conditions, relative sea level variation, or watershed practices may have upon water quality and productivity in the littoral zone. Specific questions which can be addressed within this framework are:

- What is the relationship between habitat area (i.e., areal coverage of SAV or marsh) and water quality or plant production?

- What is the impact of short term, high frequency or seasonal pulses (of a water column constituent such as total suspended solids, chlorophyll, dissolved inorganic nitrogen, or of seasonally immigrating grazers and predators) on plant production within SAV and marsh habitats? Is there a difference in modeled outcome based on the frequency of pulsed events? Is there a critical time of year for water or habitat quality?

- What is the relationship between plant production and area of habitat to the potential trophic transfer to, or production of, invertebrates and fishes?

- How do predictions for littoral zone habitats from the large scale Chesapeake Bay Program Water Quality model compare with a small scale model of SAV production and littoral zone water quality? If they differ, why and what are the implications of this?

Such questions are useful to managers both for purposes of analyzing water quality and habitat criteria as they pertain to the littoral zone and for understanding the nature of model predictions.

Our future directions include addressing specific aspects of the above questions, specific to salt marsh and eelgrass habitats, and the addition to the model of higher trophic level components for a better understanding of the losses of plant and algal production and of secondary (animal) production.

LITERATURE CITED

Baird, D. and Ulanowicz, R. E. (1989). The seasonal dynamics of the Chesapeake Bay ecosystem. *Ecological Monographs* 59, 329-364.

Boon, J. D. and Byrne, R. J. (1981). On basin hypsometry and the morphodynamic response of coastal inlet systems. *Marine Geology* 40, 27-48.

Boumans, R. M. J. and Sklar, F. H. (1990). A polygon-based spatial (PBS) model for simulating landscape change. *Landscape Ecology* 4, 83-90.

Cerco, C. and Cole, T.M. 1994. Three-dimensional eutrophication model of Chesapeake Bay: Volume 1, main report. Technical Report EL-94-4, US Army Engineer Waterways Experiment Station, Vicksburg, MS.

Childers, D. L., H.N. McKellar, R.F. Dame, F.H. Sklar, and E.R. Blood. (1993). A dynamic nutrient budget of subsystem interactions in a salt marsh estuary. *Estuarine Coastal and Shelf Science* 36, 105-131.

Christian, R. R. and Wetzel, R. L. (1991). Synergism between research and simulation models of estuarine microbial food webs. *Microbial Ecology* 22, 111-125.

Correll, D. L., Jordan, T. E. and Weller, D. E. (1992). Nutrient flux in a landscape: Effects of coastal land use and terrestrial community mosaic on nutrient transport to coastal waters. *Estuaries* 15, 431-442.

Costanza, R., F.H. Sklar, and M.L. White. (1990). Modeling coastal landscape dynamics. *BioScience* 40, 91-107.

Dame, R. F., J.D. Spurrier, T.M. Williams, B. Kjerfve, R.G. Zingmark, T.G. Wolaver, T.H. Chrzanowshi, H.N. McKellar, and F.J. Vernberg. (1991). Annual material processing by a salt marsh-estuarine basin in South Carolina, USA. *Marine Ecology Progress. Series* 72, 153-166.

de Jonge, V. N. and Colijn, F. (1994). Dynamics of microphytobenthos biomass in the Ems estuary. *Marine Ecology Progress Series* 104, 185-196.

Dennison, W. C., R.J. Orth, K.A. Moore, J.C. Stevenson, V.C. Carter, S. Kollar, P.W. Bergstrom, and R.A. Batuik. (1993). Assessing water quality with submersed aquatic vegetation. *Bioscience* 43, 86-94.

Drake, B. G. and Read, M. (1981). Carbon dioxide assimilation, photosynthetic efficiency, and respiration of a Chesapeake Bay salt marsh. *Journal of Ecology* 69, 405-423.

Eiser, W. C. and Kjerve, B. (1986). Marsh topography and hypsometric characteristics of a South Carolina salt marsh basin. *Estuarine Coastal and Shelf Science* 23, 595-605.

Finklestein, K. and Hardaway, C. S. (1988). Late holocene sedimentation and erosion of estuarine fringing marshes, York River, Virginia. *Journal of Coastal Research* 4, 447-456.

Friedrichs, C. T. and D. G. Aubrey. (1994). Uniform bottom shear stress and equilibrium hypsometry of intertidal flats. In *Mixing Processes in Estuaries and Coastal Seas* (ed. C. Pattiaratchi). Washington, D.C.: American Geophysical Union.

Gould, D. M. and Gallagher, E. D. (1990). Field measurements of specific growth rate, biomass, and primary production of benthic diatoms of Savin Hill Cove, Boston. *Limnology Oceanography* 35, 1757-1770.

Gross, M. F., M.A. Hardisky, P.L. Wolf, and V. Klemas. (1991). Relationship between aboveground and Below ground biomass of *Spartina alterniflora* (Smooth Cordgrass). *Estuaries* 14, 180-191.

Heck, K. L. and Thoman, T. A. (1984). The nursery role of seagrass meadows in the upper and lower reaches of Chesapeake Bay. 7, 531-540.

Keller, A.A. (1989). Modeling the effects of temperature, light, and nutrients on primary productivity: An empirical and a mechanistic approach compared. *Limnology and Oceanography* 34, 82-95.

Kuo, A. Y. and Park, K. (1995). A framework for coupling shoals and shallow embayments with main channels in numerical modeling of coastal plain estuaries. *Estuaries* 18, 341-350.

Lee, J. K., R.A. Park, and Paul W. Mausel. (1992). Application of geoprocessing and simulation modeling to estimate impacts of sea level rise on the northeast coast of Florida. *Photogrammetric Engineering and Remote Sensing* 58, 1579-1586.

Mallin, M. A. (1994). Phytoplankton ecology of North Carolina estuaries. *Estuaries* 17, 561-574.

Malone, T. C., W.M. Kemp, H.W. Ducklow, W.R. Boynton, J.H. Tuttle, and R.B. Jonas. (1986). Lateral variation in the production and fate of phytoplankton in a partially stratified estuary. *Marine Ecology Progress Series* 32, 149-160.

Moncreiff, C. A., M.J. Sullivan, and A.E. Daenick. (1992). Primary production dynamics in seagrass beds of Mississippi Sound: the contributions of seagrass, epiphytic algae, sand microflora, and phytoplankton. *Marine Ecology Progress Series* 87, 161-171.

Murray, L. and Wetzel, R. L. (1987). Oxygen production and consumption associated with the major autotrophic components in two temperate seagrass communities. *Marine Ecology Progress Series* 38, 231-238.

Pinckney, J. and Zingmark, R. (1993). Biomass and production of benthic microalgal communities in estuarine sediments. *Estuaries* 16, 887-897.

Rizzo, W. M., Lackey, G.J., and Christian, R.R. (1992). Significance of euphotic, subtidal sediments to oxygen and nutrient cycling in a temperate estuary. *Marine Ecology Progress Series* 86, 51-61.

Sand-Jensen, K. and Borum, J. (1991). Interactions among phytoplankton, periphyton, and macrophytes in temperate freshwaters and estuaries. *Aquatic Botany* 41, 137-175.

Spinner, G. P. (1969). Serial Atlas of the Marine Environment. In *The wildlife wetlands and shellfish areas of the Atlantic coastal zone*, vol. Folio 18. New York City: American Geographical Society.

Stevenson, J. C., L. G. Ward, and M. S. Kearney. (1988). Sediment transport and trapping in marsh systems: Implications of tidal flux studies. *Marine Geology* 80, 37-59.

Sullivan, M. J. and Moncreiff, C. A. (1988). Primary production of edaphic algal communities in a Mississippi salt marsh. *Journal of Phycology* 24, 49-58.

Sundback, K. and Graneli, W. (1988). Influence of microphytobenthos on the nutrient flux between sediment and water: a laboratory study. *Marine Ecology Progress Series* 43, 63-69.

Vorosmarty, C. J. and T. C. Loder, I. (1994). Spring-Neap tidal contrasts and nutrient dynamics in a marsh dominated estuary. *Estuaries* 17, 537-551.

Wetzel, R. L. and Neckles, H. A. (1986). A model of *Zostera marina* L. photosynthesis and growth: Simulated effects of selected physical-chemical variables and biological interactions. *Aquatic Botany* 26, 307-323.

Wetzel, R. L. and Hopkinson, C. S. (1990). Coastal ecosystem models and the Chesapeake Bay Program: Philosophy, background, and status: Virginia Institute of Marine Science.

Wetzel, R.L. and M.B Meyers. (1994). Ecosystem process modeling of submerged aquatic vegetation in the lower Chesapeake Bay. Final report (1993) to USEPA Region III Chesapeake Bay Program Office.

Wolaver, T. G., Zieman, J. C., Wetzel, R. L. and Webb, K. L. (1983). Tidal exchange of nitrogen and phosphorus between a mesohaline vegetated marsh and the surrounding estuary in the lower Chesapeake Bay. *Estuarine Coastal and Shelf Science* 16, 321-332.

Appendix A. List of auxiliary equations for the four littoral zone habitat models of the Goodwin Islands National Estuarine Research Reserve. The formulations for diatoms and other plankton are similar. The formulations for labile and particulate organic carbon are also similar. Please refer to Wetzel and Neckles (1986) for formulations related to Zostera marina and epiphytic carbon production.

Diatom Gross Production (gC d^{-1})

$$Dia_{TT} = Dia_{hab} * diaPmax * DiaPTctrl * DiaG_{lim}$$

Diatom Photosynthesis Temperature Control (unitless)

$$DiaPTctrl = e^{(-DiaPT1 * (T_{water} - DiaPTopt))} \quad (if\ T_{water}\ DiaPTopt)$$

$$= e^{(-DiaPT2 * (DiaPTopt - T_{water}))} \quad (if\ T_{water}\ DiaPTopt)$$

Diatom Growth Limitation (unitless)

$$DiaG_{lim} = MAX(DiaN_{lim}, DiaI_{lim}) \quad (If\ PAR_0 > 0.0)$$

Diatom Irradiance Control (unitless)

$$DiaI_{lim} = \frac{PAR_{hab}}{(PAR_{hab} + DiaIK)}$$

Diatom Nitrogen Limitation Function (unitless)

$$DiaN_{lim} = \frac{TDIN_{hab}}{(TDIN_{hab} + DiaKDIN)}$$

Diatom Respiration (gC d^{-1})

$$Dia_{resp} = Dia_{hab} * DiaRTctrl$$

Diatom Respiration Control with Temperature (d^{-1})

$$DiaRTctrl = BMRd * e^{(KtBd * (T_{water} - DiaRTopt))}$$

Diatom Mortality (gC d^{-1})

$$Dia_{mort} = Dia_{hab} * DiaMTctrl$$

Diatom Mortality Control with Temperature (d^{-1})

$$DiaMTctrl = PPRd * e^{(KtBd * (T_{water} - DiaRTopt))}$$

Diatom Exudation (gC d^{-1})

$$Dia_{exu} = Dia_{prod} * DiaExuK$$

Diatom Sedimentation (gC d $^{-1}$)

$$Dia_{sed} = \frac{Dia_{hab} * DiaSedK}{h_{hab}}$$

Total POC Production (gC d-1)

$$TPOC_{TI} = PhytoPOCf * (Dia_{mort} + OP_{mort}) + SM_{resus}$$

Labile POC Production (gC d-1)

$$LPOC_{prod} = FLPOC * TPOC_{prod}$$

Labile POC Hydrolysis (gC d-1)

$$LPOC_{hydrol} = LPOC_{hab} * KLC * HydrolTC$$

$$HydrolTC = e^{(KHydrol * (T_{water} - TrHydrol))}$$

Labile POC Settling (gC d-1)

$$LPOC_{set} = \frac{LPOC_{hab} * StlV_{det}}{h_{hab}}$$

Total DOC Production (gC d-1)

$$TDOC_{prod} = (LPOC_{hydrol} + RPOC_{hydrol}) + (Dia_{exu} + OP_{exu})$$

Total DOC Remineralization (gC d-1)

$$DOC_{remin} = DOC_{hab} * KDC * (1 - FRDOC) * ReminTC$$

$$ReminTC = e^{(KRemin * (T_{water} - TrRemin))}$$

Total DIN Production (mmoleN d^{-1})

$$TDIN_{prod} = DOC_{remin} * \frac{1000}{DOMCN * 14}$$

Total DIN Uptake (mmoleN d^{-1})

$$TDIN_{uptake} = DiaN_{upt} + OPN_{upt}$$

$$TDIN_{VSTuptake} = DiaN_{upt} + OPN_{upt} + ZSHN_{upt}$$

Total DIN Sediment Water Flux (mmoleN d-1)

$$TDIN_{swflx} = TDINflx_{mthavg} \quad (If\ PAR_o > 0.0)$$

Sediment Microalgae Carbon Loss Through Grazing (gC m^{-2} d^{-1})

$$SMC_{los} = (SMMK * SMC^2)$$

Sediment Microalgae Carbon Loss Through Resuspension (gC m^{-2} d^{-1})

$$SMC_{res} = SMC * SMresK$$

Zostera marina Shoot Nitrogen Uptake (gN m^{-2} d^{-1})

$$ZSN_{uptake} = ZSN * ZSNmm$$

Zostera marina Shoot Nitrogen Uptake (gN gN^{-1} d^{-1})

$$ZSNmm = ZSCNfb * ZSC_{relgro} * ZSVmN * \left(\frac{TDIN_{hab}}{TDIN_{hab} + ZSKs}\right)$$

Zostera marina Shoot C:N Feedback Function (unitless)

$$ZSCNfb = \frac{ZSCN - ZSCNmin}{ZSCNmax - ZSCNmin} \quad \left(where\ ZSCN = \frac{ZSC}{ZSN}\right)$$

Zostera marina Shoot Relative Growth (unitless)

$$ZSC_{relgro} = \frac{ZS_{photo}}{ZPT}$$

Zostera marina Nitrogen Translocation from Root-Rhizomes to Shoots (gN m^{-2} d^{-1})

$$ZN_{trans} = (ZSN_{demand} - ZSN_{uptake}) * (ZSCNfb) * (1 - ZRRCNfb)$$

Zostera marina Shoot Nitrogen Demand (gN m^{-2} d^{-1})

$$ZSN_{demand} = \frac{ZSC_{net}}{ZSCNopt}$$

Zostera marina Shoot Nitrogen Loss (gN m^{-2} d^{-1})

$$ZSN_{los} = \frac{ZSC}{ZSCN}$$

Appendix B. Complete list of parameters for the four littoral zone habitat models of the Goodwin Islands National Estuarine Research Reserve.

Temporal and Spatial Considerations

JD	Julian Day	d	
dt	Integration Stepsize (Subtidal)	d	0.03125
	Integration Stepsize (Intertidal)	d	0.0078125
modhrs	Continuous Model Time in Hours	h	
thours	Daily Model Time in Hours	h	
Area	Habitat and Ecosystem Areas	m^2	

Habitat Depth Parameters

Abbreviation	Description	Units	Value
MSL	Mean Sea Level	m	0.00
hfilm	Intertidal Permanent Water Film Thickness	m	0.01
zNVST	NonVeg Subtidal Reference Elevation	m	-1.88
zVST	VegSubtidal Reference Elevation	m	-0.88
zNVIT	NonVeg Intertidal Reference Elevation	m	-0.36
zVIT	Veg Intertidal Reference Elevation	m	-0.00
$Area_{NVST}$	NonVeg Subtidal Wetted Area	m^2	420e04
$Area_{VST}$	Veg Subtidal Wetted Area	m^2	120e04
$Area_{NVIT}$	NonVeg Intertidal Maximum Wetted Area	m^2	100e04
$Area_{VIT}$	Veg Intertidal Maximum Wetted Area	m^2	85e04

Irradiance Attenuation Parameters

Abbreviation	Description	Units	Value
Kwater	PAR attenuation constant for Water	m^{-1}	0.04
POCatn	PAR attenuation due to Suspended Detritus	$m^2\ gC^{-1}$	0.14
DOCatn	PAR attenuation due to water column DOC	$m^2\ gC^{-1}$	0.14
Chlatn	PAR attenuation due to water column Chla	$m^2\ mgChla^{-1}$	0.0138
aZm	Vertical PAR attenuation due to Zostera marina biomass	$m^2\ gC^{-1}$	0.002
aSa	Vertical PAR attenuation due to Spartina alterniflora biomass	$m^2\ gC^{-1}$	0.002

Boundary Concentration Parameters

Abbreviation	Description	Units	Value
ChanDiaC	Channel Diatom C Concentration	$gC\ m^{-3}$	variable
ChanOPC	Channel Other Plankton C Concentration	$gC\ m^{-3}$	variable
ChanDOC	Channel DOC Concentration	$gC\ m^{-3}$	0.7

ChanLPOC	Channel Labile POC Concentration	gC m^{-3}	2.75
ChanRPOC	Channel Refractory POC Concentration	gC m^{-3}	2.25
ChanTDIN	Channel Total DIN Concentration	μM	20.0
NVSTDiaC	NonVeg Subtidal Diatom C Concentration	gC m^{-3}	0.165
NVSTOPC	NonVeg Subtidal Other Plankton C Concentration	gC m^{-3}	0.330
NVSTLPOC	NonVeg Subtidal Labile POC Concentration	gC m^{-3}	2.75
NVSTRPOC	NonVeg Subtidal Refractory POC Concentration	gC m^{-3}	2.25
NVSTDOC	NonVeg Subtidal DOC Concentration	gC m^{-3}	0.7
NVSTDIN	NonVeg Subtidal DIN Concentration	μM	10.0
VSTDiaC	Veg Subtidal Diatom C Concentration	gC m^{-3}	0.165
VSTOPC	Veg Subtidal Other Plankton C Concentration	gC m^{-3}	0.330
VSTLPOC	Veg Subtidal Labile POC Concentration	gC m^{-3}	2.75
VSTRPOC	Veg Subtidal Refractory POC Concentration	gC m^{-3}	2.25
VSTDOC	Veg Subtidal DOC Concentration	gC m^{-3}	0.7
VSTDIN	Veg Subtidal DIN Concentration	μM	10.0
NVITDiaC	NonVeg Intertidal Diatom C Concentration	gC m^{-3}	0.165
NVITOPC	NonVeg Intertidal Other Plankton C Concentration	gC m^{-3}	0.330
NVITLPOC	NonVeg Intertidal Labile POC Concentration	gC m^{-3}	2.75
NVITRPOC	NonVeg Intertidal Refractory POC Concentration	gC m^{-3}	2.25
NVITDOC	NonVeg Intertidal DOC Concentration	gC m^{-3}	3.5
NVITDIN	NonVeg Intertidal DI Concentration	μM	5.0
VITDiaC	Veg Intertidal Diatom C Concentration	gC m^{-3}	0.165
VITOPC	Veg Intertidal Other Plankton C Concentration	gC m^{-3}	0.330
VITLPOC	Veg Intertidal Labile POC Concentration	gC m^{-3}	2.75
VITRPOC	Veg Intertidal Refractory POC		

	Concentration	$gC\ m^{-3}$	2.25
VITDOC	Veg Intertidal DOC Concentration	$gC\ m^{-3}$	3.5
VITDIN	Veg Intertidal DIN Concentration	μM	5.0

Global Algal Rate Parameters

Abbreviation	Description	Units	Value
OPttlPhyto	Other Plankton:Total Phytoplankton	unitless	0.67
CChla	Diatom and OP Carbon:Chla	unitless	50.0
PPOCf	Fraction of Phyto Mort to POC	unitless	0.80
BMRd	Diatom Basal Metabolic Rate	d^{-1}	0.015
KtBd	Constant for Diatom Respiration Temperature Function	$°C^{-1}$	0.069
DIAExK	Diatom Exudation Constant	unitless	0.30
DIAPT1	Diatom Photosynthesis Temperature Coefficient 1	unitless	0.004
DIAPT2	Diatom Photosynthesis Temperature Coefficient 2	unitless	0.006
DIASdK	Diatom Sedimentation Coefficient	$m\ d^{-1}$	0.25
DIACN	Diatom C:N Ratio (weight)	unitless	5.7
DIAIK	Diatom Half-Saturation Constant for Photosynthesis	$\mu E\ m^{-2}\ s^{-1}$	140
DIAKsN	Diatom Half-Saturation Constant for Nitrogen Uptake	μM	10.0
DIAPmax	Diatom Maximum Photosynthetic Rate	d^{-1}	0.50
DIAPTopt	Reference Temperature for Diatom Photosynthesis	°C	20.0
DIARTopt	Reference Temperature for Diatom Respiration	°C	20.0
PRRd	Predation Rate on Diatoms (Mortality)	d^{-1}	0.15
BMRop	Other Plankton Basal Metabolic Rate	d^{-1}	0.015
KTBop	Constant for OP Respiration Temperature Function	$°C^{-1}$	0.069
OPExK	Other Plankton Exudation Constant	unitless	0.30
OPSdK	Other Plankton Sedimentation Constant	$m\ d^{-1}$	0.10
OPCN	Other Plankton C:N (weight)	unitless	5.7
OPIK	Other Plankton Half-Saturation Constant for Photosynthesis	$\mu E\ m^{-2}\ s^{-1}$	140
OPKDin	Other Plankton Half-Saturation Constant for Nitrogen Uptake	μM	10.0
OPPmax	Other Plankton Maximum Photosynthetic Rate	d^{-1}	0.50
OPPTopt	Reference Temperature for Other Plankton Photosynthesis	°C	25.0

OPRTopt	Reference Temperature for Other Plankton Respiration	°C	20.0
OPPT1	Other Plankton Photosynthesis Temperature Coefficient 1	unitless	0.008
OPPT2	Other Plankton Photosynthesis Temperature Coefficient 2	unitless	0.010
PRRop	Predation Rate on Other Plankton	d^{-1}	0.15
SMCNopt	Sediment Microalgae optimal C:N	unitless	5.7
SMIK	Sediment Microalgae Half Saturation Constant for Photosynth.	$\mu E\ m^{-2}\ s^{-1}$	100
SMPmax	Sediment Microalgae Maximum Photosynthetic Rate	d^{-1}	0.576
BMRsm	Sediment Microalgae Basal Respiration Rate	d^{-1}	0.05
KtBsm	Constant for Sediment Microalgae Respiration Temperature Function	$°C^{-1}$	0.069
SMRTopt	Reference Temperature for Sediment Microalgae Respiration	°C	20.0
SmMK	Sediment Microalgal Mortality Constant	$m^2\ gC^{-1}\ d^{-1}$	0.045
SmJDm	Sediment Microalgae Julian Day Mortality	day	45
SMResK	Sediment Microalgae Resuspension Constant	d^{-1}	0.05

Global Kinetic Parameters

Abbreviation	Description	Units	Value
$StlV_{det}$	Detritus Settling Velocity	$m\ d^{1}$	0.25
DOMCN	Dissolved OM C:N ratio	unitless	10.0
POMCN	Particulate OM C:N ratio	unitless	10.0
DOMCN	Dissolved OM C:N ratio	unitless	10.0
FLPOC	Labile POC Fraction	unitless	0.55
FRDOC	Refractory DOC Fraction	unitless	0.00*
FRPOC	Refractory POC Fraction	unitless	0.45
KDC	Constant for DOC Remineralization	d^{-1}	0.01
KLC	Constant for LPOC Hydrolysis	d^{-1}	0.075
KRC	Constant for RPOC Hydrolysis	d^{-1}	0.005
Khydrol	Constant for POC Hydrolysis. Temperature Function	$°C^{-1}$	0.069
Kremin	Constant for DOC Remin. Temperature Function	$°C^{-1}$	0.069
TrHydrol	Reference Temperature for POC Hydrolysis	°C	20.0
TrRemin	Reference Temperature for DOC Remineralization	°C	20.0

Zostera Related Parameters

Abbreviation	Description	Units	Value
ZCpot	Potential Fraction of Zostera Shoot Production Translocated	unitless	0.25
ZfPOCdep	Potential Fraction of Zostera Shoot POC deposited	unitless	0.50
ZJDm	Zostera Shoot Fall JD Mortality	unitless	333
ZSFMK	Zostera Shoot Fall Mortality Constant	d^{-1}	0.0135
Zsmk1	Zostera Shoot Mortality Coefficient 1	unitless	0.0003
Zsmk2	Zostera Shoot Mortality Coefficient 1	unitless	0.0005
Zsmax	Zostera Shoot Maximum Biomass	$gC\ m^{-2}$	200
ZSlim	Zostera Shoo Limitation Concentration	$gC\ m^{-2}$	100
ZSCDW	Zostera Shoot Carbon Content	$gC\ gdw^{-1}$	0.40
ZSCNmax	Zostera Shoot Maximum C:N (weight)	unitless	22
ZSCNmin	Zostera Shoot Minimum C:N (weight)	unitless	12
ZSCNopt	Zostera Shoot Optimal C:N (weight)	unitless	16
ZSKsN	Zostera Shoot Half Saturation Constant for N Uptake	μM	10
ZSVmN	Zostera Shoot Maximum Nitrogen Uptake Rate	d^{-1}	0.021
ZRRmax	Zostera Root-rhizome Biomass Maximum	$gC\ m^{-2}$	200
ZRRlim	Zostera Root-rhizome Density Limitation Concentration	$gC\ m^{-2}$	100
ZRRCNmax	Zostera Root-rhizome Maximum C:N ratio (weight)	unitless	28
ZRRCNmin	Zostera Root-rhizome Minimum C:N ratio (weight)	unitless	15
ZRRCNopt	Zostera Root-rhizome Optimal C:N ratio (weight)	unitless	25
ZRRKsN	Zostera Root-rhizome Half Saturation Constant for N Uptake	μM	30
ZRRR@20	Zostera Root-rhizome Respiration Rate at 20 °C	d^{-1}	0.0005
ZRRRK	Zostera Root-rhizome Respiration Constant	unitless	1.25
ZRRTref	Zostera Root-rhizome Metabolic Reference Temperature	°C	20.0

ZRRVmN	Zostera Root-rhizome Maximum Nitrogen Uptake Rate	d^{-1}	0.072
ZRRbk	Zostera Root-rhizome Bed Storage Constant	unitless	0.05
BMRZepi	Zostera Epiphyte Basal Metabolic Rate	d^{-1}	0.045
KtBZepi	Constant for Zostera Epiphyte Respiration Temperature Function	$°C^{-1}$	0.069
ZepiGK	Zostera Epiphyte Grazing Constant	$m^2\ gC^{-1}\ d^{-1}$	0.001
ZEpiRTopt	Reference Temperature for Zostera Epiphyte Respiration	°C	20.0

Spartina Related Parameters

Abbreviation	Description	Units	Value
Scgdw	Spartina Shoot Carbon Content	$gC\ gdw^{-1}$	0.40
SCTpot	Spartina Maximum Fractional Downward Carbon Translocation	unitless	0.75
SfPOCdep	Fraction of Spartina Shoot Carbon to Sediment POC Pool	unitless	0.90
SIK	Half Saturation Constant for Spartina Photosynthesis	$\mu E\ m^{-2}\ s^{-1}$	265
SPmax	Spartina Maximum Photosynthetic Rate	d^{-1}	0.15
SSC_{bmort}	Spartina Shoot Basal Mortality	d^{-1}	0.00375
SSCNmax	Spartina Shoot Maximum C:N ratio (weight)	unitless	30
SSCNmin	Spartina Shoot Minimum C:N ratio (weight)	unitless	20
SSCNopt	Spartina Shoot Optimum C:N ratio (weight)	unitless	
SSR@20	Spartina Shoot Respiration at 20 °C	d^{-1}	0.01
SSRK	Spartina Shoot Respiration Constant	unitless	1.07
SSRTref	Spartina Shoot Metabolic Reference Temperature	°C	20.0
SSPK1	Spartina Shoot Spring Pulse Constant 1	unitless	0.025
SSPK2	Spartina Shoot Spring Pulse Constant 2	unitless	0.025
SSPJD	Spartina Shoot Spring Pulse Julian Day	unitless	115
SSprmax	Spartina Shoot Spring Pulse Maximum	d^{-1}	0.01
SSJDm	Spartina Shoot Mortality Onset Julian Day	unitless	190
SSTK1	Spartina Shoot Photosynthesis Temperature Constant 1	unitless	0.005

SSTK2	Spartina Shoot Photosynthesis Temperature Constant 2	unitless	0.002
SPTopt	Spartina Shoot Photosynthesis Temperature Control	°C	20
SRRCmax	Spartina Root-Rhizome Maximum Biomass	$gC\ m^{-2}$	1000
SRRCmin	Spartina Root-Rhizome Minimum Biomass	$gC\ m^{-2}$	500
SRRKsN	Half Saturation Constant for N Uptake by Spartina Root-Rhizomes	μM	100
SRRmK	Spartina Root-Rhizome Loss Constant	unitless	1.25
SRRM@20	Spartina Root-Rhizome Loss Rate at 20 °C	d^{-1}	0.0006
SRRCNmax	Spartina Root-Rhizome Maximum C:N ratio (weight)	unitless	300
SRRCNmin	Spartina Root-Rhizome Minimum C:N ratio (weight)	unitless	80
SRRCNopt	Spartina Root-Rhizome Optimal C:N ratio (weight)	unitless	200
SRRR@20	Spartina Root-Rhizome Respiration Rate at 20 °C	d^{-1}	0.0006
SRRRK	Spartina Root-Rhizome Respiration Constant	unitless	1.25
SRRTref	Spartina Root-Rhizome Metabolic Reference Temperature	°C	20.0
SRRbk	Spartina Root-Rhizome Bed Storage Constant	unitless	0.075
SRRVmN	Spartina Root-Rhizome Maximum Nitrogen Uptake Rate	d^{-1}	0.134